Analyst

PAPER

View Article Online
View Journal | View Issue

Cite this: *Analyst*, 2019, **144**, 1582

A graphene oxide/gold nanoparticle-based amplification method for SERS immunoassay of cardiac troponin I†

Xiuli Fu,[a] Yunqing Wang,[b] Yongming Liu,[a] Huitao Liu,[a] Longwen Fu,[b] Jiahui Wen,[a] Jingwen Li,[a] Peihai Wei[c] and Lingxin Chen *[a,b]

Cardiac troponin I (cTnI) was considered as the "gold standard" for acute myocardial infarction (AMI) diagnosis owing to its superior cardiac specificity for cardiac damage and showing little or no changes in patients with a skeletal muscle disease or trauma. Herein, a new signal amplification surface-enhanced Raman scattering (SERS) platform was developed for recognition and detection of cTnI by using gold nanoparticles (AuNPs), graphene oxide (GO) and magnetic beads (MB). Here, antibody/Raman reporter labeled AuNP–functionalized GO were employed as both SERS nanotags and signal amplification carriers. Monoclonal antibody modified MB were applied as the capture probe and separation agents. In the presence of cTnI, sandwich type immunocomplexes, "capture probe/target/SERS nanotags", were formed through antibody–antigen–antibody interactions. Due to the strong SERS enhancement ability of the designed GO/AuNP complexes and a high binding chance between cTnI and the GO/AuNP complexes, the proposed SERS-based immunoassay could selectively detect cTnI with a high sensitivity (detection limit of 5 pg mL^{-1}) and a good linearity was obtained in a range of 0.01–1000 ng mL^{-1}. In addition, this method was also successfully applied for detecting cTnI in serum substitute media with a similar linear range. Furthermore, this strategy can be constructed with different kinds of antibodies and Raman reporters, and thus can be easily used for simultaneous detection of multiple biomarkers. Therefore, this proposed SERS-based signal amplification technique shows strong potential for the clinical diagnosis of AMI disease.

Received 21st October 2018,
Accepted 27th December 2018

DOI: 10.1039/c8an02022a

rsc.li/analyst

Introduction

Acute myocardial infarction (AMI) has been one of the leading causes of death for both men and women in the world, due to reduced blood supply to the heart.[1,2] In this case, rapid identification and diagnosis of AMI are critical for the initiation of effective medical treatment and management. Up to now, electrocardiography (ECG) has been the primary method for measurement and diagnosis of AMI. However, not all of the patients with AMI exhibit electrocardiographic changes, and ECG has the limitation of low sensitivity[1,3,4] To overcome the issues with ECG, an alternative strategy is expected for the detection of AMI. Accordingly, AMI could be diagnosed *via* different kinds of cardiac biomarkers, including cardiac troponin I (cTnI), cardiac troponin T (cTnT), creatine kinase-MB and myoglobin.[4,5] Compared with other biomarkers of AMI, cTnI has superior cardiac specificity for cardiac damage, while showing little or no changes in patients with a skeletal muscle disease or trauma.[3,6–9] Based on the above, cTnI has been recognized as the "gold standard" for AMI diagnosis. Thus, a rapid and sensitive method to confirm AMI using cTnI is desirable, which has the great potential to prevent sudden death due to cardiac disease.

Previously many methods have been used for cTnI detection and quantification, such as enzyme-linked immunosorbent assay (ELISA),[10] chemiluminescence immunoassays,[11,12] fluorescence immunoassays,[13–15] electrical detection,[16] surface plasmon resonance detection (SPR),[17,18] colorimetric protein array,[19] naked eye[20] and so on. However, the major limitation in currently used cTnI assays is low sensitivity and precision at the time of a patient's presentation, owing to a delayed increase in circulating levels of cardiac troponin.

[a]*School of Chemistry and Chemical Engineering, Yantai University, Yantai 264005, China*
[b]*Key Laboratory of Coastal Environmental Processes and Ecological Remediation, Yantai Institute of Coastal Zone Research, Chinese Academy of Sciences, Yantai 264003, China. E-mail: lxchen@yic.ac.cn; Fax: +86-535-2109130; Tel: +86-535-2109130*
[c]*School of Chemistry and Chemical Engineering, Qilu Normal University, 36 Lishan Road, Jinan 250013, China*

†Electronic supplementary information (ESI) available. See DOI: 10.1039/c8an02022a

Therefore, this calls for a highly sensitive method for detecting cTnI.

Up to now, various techniques and methods have been established for improving the detection sensitivity through a signal amplification strategy.[21–28] For example, to improve the poor sensitivity of conventional ELISA, Wu *et al.* designed a gold nanoparticle (AuNP)-based enzyme-linked antibody–aptamer sandwich strategy for quantification of *Salmonella enterica* serovar Typhimurium.[22] Zhou *et al.* employed a matched nanobody pair and a π–π stacked graphene oxide/thionine hybrid-based probe for detection of Cry1C (a kind of toxin protein).[24] Wang's group has reported the detection of microRNAs based on amplified silver deposition using alkaline phosphatase-incorporated gold nanoclusters[25] or by the synergic combination of TiO_2 photocatalysis and guanine photoreduction.[26] Besides, different enzyme mimic nanocomplexes have been fabricated by using graphene oxide dispersed carbon nanotubes for enhanced peroxidase-like catalytic and electrocatalytic activities.[27,28] Recently, a Surface-Enhanced Raman Scattering (SERS)-based immunoassay technique using a functional nanomaterial as SERS nanotags is emerging as a powerful candidate to resolve the low sensitivity problem.[29–31] The detection sensitivity of the SERS technique can be enhanced up to 10–14 orders of magnitude higher than that of conventional Raman spectroscopy when reporter molecules are adsorbed on or near the surface of a nanoparticle.[32–34] This enhancement is due to the electromagnetic and chemical enhancement effects, which are dependent on the composition, size, shape and aggregation of the nanoparticles.[33,34] Meanwhile, AuNPs are most widely used as a SERS enhancing agent owing to their long-term stability, controllable size distribution, easy preparation and modification, and good biocompatibility with biomolecules such as antibodies and aptamers.[35,36] However, in spite of the excellent properties of AuNPs, the SERS enhancement effect of a single nanoparticle is a major hurdle for the sensitive detection of a specific target. Thus, it is necessary to combine AuNPs with other nanomaterials. Graphene oxide (GO) is a novel, one-atom thick, two-dimensional carbon nanomaterial that has drawn intense attention in the fields of modern analytical chemistry due to its unique structure and easy conjugation with other nanoparticles and/or biomolecules without degrading their native properties.[37–39]

Herein, we established a new SERS platform using GO/AuNP conjugates as the SERS nanotags based on the signal amplification strategy for highly sensitive and selective detection of cardiac biomarkers cTnI. For this purpose, we created antibody/Raman reporter (malachite green isothiocyanate (MGITC)) modified AuNPs and further conjugated with GO as the SERS nanotags to generate highly sensitive SERS signals. Then, we designed monoclonal antibody functionalized magnetic beads (MB) as the capture probe and separate substrates. Comparing with the use of two-dimensional planar substrates, the MB-based sensor technique avoided the low immunoreaction problems caused by the diffusion-limited kinetics. Here, the sandwich-type immunocomplexes "capture probe/target/SERS nanotags" were formed based on the "antibody–antigen–antibody" interactions. The strong affinity between the antibody and antigen assured the specificity of this system. This proposed method is expected to provide new insights into the early diagnosis of AMI disease.

Experiment section

Materials and instruments

Graphene oxide was purchased from Nanjing XFNano Materials Technology Company (Nanjing, China). Gold(III) chloride trihydrate (>99.9%), sodium citrate dehydrate (99%), bovine serum albumin (BSA), 1-ethyl-3-(3-dimethylaminopropyl) carbodiimide hydrochloride (EDC), *N*-hydroxysuccinimide (NHS), sodium hydroxide, hydrochloric acid and sodium chloroacetate were purchased from Sigma-Aldrich. Carboxylated magnetic beads with a diameter of 1 μm, malachite green isothiocyanate (MGITC) and phosphate buffer saline (PBS, pH 7.4) were purchased from Invitrogen Corporation (USA). Human cardiac troponin I (cTnI), mouse monoclonal antibodies to cTnI (Capture cTnI), and rabbit polyclonal antibodies to cTnI were obtained from Abcam (UK). Serum substitute media (SeraSub) were obtained from CST Technologies, Inc. All antigens and antibodies were aliquoted, refrigerated at −20 °C, and treated according to the manufacturer's guidelines. All reagents were used as received without further purification. Aqueous solutions were prepared with freshly deionized water (18.2 MΩ specific resistance) obtained from a Milli-Q system (Millipore S.A., Bedford, USA).

SERS measurements were performed using a Renishaw inVia Raman microscope system (Renishaw, UK). A Spectra-Physics He–Ne laser operating at λ = 633 nm was used as the excitation source with a power of 20 mW. Raman scattering was observed using a charge-coupled device (CCD) camera with a spectral resolution of 4 cm^{-1}. A 20× objective lens was employed to focus a laser spot on the sandwich immunocomplexes in a capillary tube. Raman signals were collected using a 1 s exposure time with 1 time accumulation. All SERS spectra were calibrated referring to the 520 cm^{-1} silicon line. The WiRE 4.0 software was employed to control the instrument and for data acquisition. UV-visible absorption spectra were obtained using a Cary 100 spectrophotometer (Varian, USA). High-magnification transmission electron micrographs (TEM) were obtained using a JEOL JEM 2100F instrument at an accelerating voltage of 200 kV. Dynamic light scattering (DLS) data of the NPs were obtained using a Nano-ZS90 (Malvern).

Preparation of SERS nanotags

AuNPs were prepared using the citrate-reduction method reported by Frens.[40] Briefly, 50 mL 0.01% gold(III) chloride trihydrate solution was brought to boil with vigorous stirring in a round-bottom flask fitted with a reflux condenser, and then 0.5 mL of 1% tri-sodium citrate solution was added rapidly to the solution. After the solution was boiled for another 15 min, heating was stopped and the solution was stirred for 1 h. The

resulting solution was cooled to room temperature and stored at 4 °C. The final concentration of the AuNP solution was calculated to be 0.12 nM. UV-vis spectroscopy and DLS were used to identify the average size of gold nanoparticles (Fig. S1†). Our measurements estimated the average diameter of gold particles to be 40 nm.

Then, 1 μL of 10^{-4} M MGITC was added to 1.0 mL of 0.12 nM AuNPs, and the mixture was reacted for 30 min under stirring. The number of adsorbed MGITC molecules per particle was estimated to be 833, which was calculated from the amount of MGITC (1 μL, 10^{-4} M) and AuNPs (1 mL, 0.12 nM). After that, the antibody conjugates were prepared according to the literature with slight modifications.[41] Here, the rabbit polyclonal antibody to cTnI was used as the detection antibody. Before detection antibody conjugation, the MGITC functionalized AuNPs were adjusted to pH 9.0. After that, 2 μL of 1 mg mL^{-1} detection antibody was added into 1 mL of pH-adjusted MGITC functionalized AuNP suspension followed by incubation at room temperature (RT) for 2 h with gentle stirring. During this time, the detection antibodies were adsorbed onto the surface of AuNPs through a combination of ionic and hydrophobic interactions. Then, after being blocked with 100 μL of 10% BSA solution for 30 min at RT, the antibody/MGITC functionalized AuNPs were centrifuged at 7400 rpm for 10 min, and the process was repeated three times. The clear supernatant was carefully removed, and the precipitated gold conjugates were resuspended in 100 μL of PBS containing 1% BSA and stored at 4 °C. UV-Vis spectroscopy, DLS and SERS were used to identify the conjugation between the antibody and MGITC functionalized AuNPs. Fig. S2A† showed that the UV-vis absorption band for antibody/MGITC conjugated AuNPs was slightly shifted from 530 nm to 532 nm. In addition, the average diameter of MGITC functionalized AuNPs increased from 43 nm to 55 nm after conjugation with the antibody as shown in Fig. S2B.† SERS spectra also demonstrated that the capture probe could display strong Raman signals only after conjugation with the antibody/MGITC functionalized AuNPs (Fig. S2C†). All these results demonstrated that the antibody was successfully conjugated with the MGITC functionalized AuNPs.

Finally, the SERS nanotags were prepared by following a published procedure.[42,43] To obtain a nano-sized GO aqueous suspension (1 mg mL^{-1}), GO was cracked with an ultrasonic probe at 200 W for 120 min. After sonication, the size of GO was around 100–200 nm (Fig. S3A, B†). Then, 50 mg of NaOH and $ClCH_2COONa$ were added to the GO suspension and bath sonicated for 2 h to convert the OH groups to COOH groups. The resulting dispersion was neutralized with dilute hydrochloric acid and purified by repeated rinsing and centrifugation until the product was well dispersed in deionized water. Then the final product was dispersed into 1 mL of pH 6.0 MES buffer containing 400 mM EDC and 200 mM NHS to obtain a homogeneous black suspension by 30 min activation. Excess EDC and NHS were separated by centrifugation at 10 000 rpm for 5 min, and the precipitate was washed 3 times with PBS buffer and resuspended in 1.0 mL of pH 7.4 PBS buffer. Next, the antibody/MGITC functionalized AuNPs were added and the mixture was stirred for 4 h at RT. After centrifugation and washing 3 times, the resulting SERS nanotags were redispersed in 4.0 mL of PBS containing 1% BSA and stored at 4 °C. The TEM images of SERS nanotags are displayed in Fig. S3C.† The image shows that the antibody/MGITC functionalized AuNPs are attached on the surface of GO through the antibody after modification.

Preparation of antibody-functionalized magnetic beads (capture probe)

For the activation of the COOH terminal groups on the magnetic beads, 10 μL of 0.1 M NHS and 10 μL of 0.1 M EDC were added to 1.0 mL of 0.5 mg mL^{-1} magnetic beads and allowed to react for 30 min. Unreacted EDC and NHS were separated by magnetic decantation. The resultant particles were redispersed in 1 mL of PBS buffer at pH 7.4. Then, 10 μL of 1 mg mL^{-1} mouse monoclonal anti-cTnI was added to the activated magnetic beads and reacted for 2 h. Following that, 10 μL of 10% BSA in PBS was injected into the suspension and incubated for 30 min to block the possible residual sites on the MB. Afterward, unreacted chemicals were removed using a micropipette after immobilization of the magnetic beads by the use of a magnetic bar and the obtained pellet was resuspended into 1 mL of PBS (pH 7.4) containing 1.0% BSA and stored at 4 °C for further usage.

SERS-based immunoassay for the determination of cTnI

Aliquots of the antibody-functionalized magnetic bead (capture probe) suspension were added into 1.5 mL centrifuge tubes and aliquots of cTnI standards with various concentrations (0–1000 ng mL^{-1}) were then introduced into each centrifuge tube. After incubation for 2 h at RT, the mixture was separated simply with an external magnet and washed with PBS. Following that, aliquots of SERS nanotags were added into each tube. After incubation for 1 h, the sandwich immunocomplexes (capture probe/cTnI/SERS nanotags) were formed. These magnetic immunocomplexes were isolated and washed as per the above protocol. Then, the immunocomplexes were redispersed in 10 μL PBS buffer. Finally, the remaining supernatant solution was transferred into a capillary tube for SERS detection.

For the method without GO, different concentrations of cTnI were prepared and incubated with antibody-functionalized magnetic beads for 2 h at RT. After the washing step, the antibody/MGITC functionalized AuNPs were added and further incubated for another 2 h. All the samples were analyzed according to the same procedure as that of the method with GO mentioned above.

Serum sample preparation

In order to evaluate the practicality of the developed SERS sensing platform, aliquots of SeraSub were spiked with standard cTnI solutions to result in various final concentrations (0–1000 ng mL^{-1}). All the serum samples with and without

spiking were analyzed according to the same procedure as that of the standard solution analysis mentioned above.

Results and discussion

Sensing strategy

Fig. 1 presents the assay principle of the enhanced SERS immunoassay based on the antibody/Raman reporter labeled AuNP–functionalized GO amplification strategy. Here, monoclonal antibody immobilized MB were utilized as the capture probe for targeting cTnI and employed to separate immune conjugates. Antibody/MGITC labeled AuNP–functionalized GO were employed as both SERS nanotags and signal amplification carriers. In this work, one GO sheet could carry lots of detection antibodies due to the conjugation with antibody/MGITC labeled AuNPs. Thus the binding chance between the target and our SERS nanotags was significantly enhanced owing to the increasing ratio of the detection antibody to target. Meanwhile, through the conjugation process between GO and functionalized AuNPs, the distances between functionalized AuNPs were shortened, which caused a certain degree of aggregation, and then resulted in a number of 'hot spots'. Due to the above, the Raman signals were greatly enhanced. As expected from the original design, in the presence of cTnI, the cTnI was captured by the antibody on the surface of MB, and then conjugation with SERS nanotags occurred. In this case, the sandwich type "capture probe/cTnI/SERS nanotag" immunocomplex formed, which resulted in a strong SERS signal as illustrated in Fig. 2b. In contrast, in the absence of cTnI, the SERS nanotags could not bind with antibody functionalized MB, which displayed very low or no SERS signal, as seen in Fig. 2a. Hence, the changes in the SERS signal were expected to provide a quantitative readout for detection of cTnI. This phenomenon was further confirmed by TEM images that lots of GO/AuNP complexes appeared on the surface of antibody-functionalized MB in the presence of cTnI while no GO/AuNP complexes were observed in the absence of cTnI (Fig. 2a and b).

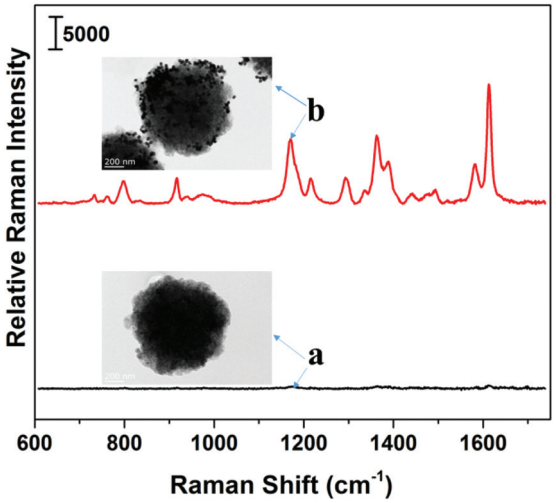

Fig. 2 Typical SERS spectra and TEM images of the capture probe (antibody functionalized magnetic bead) in the absence (a) and presence (b) of cTnI (500 ng mL^{-1}, scale bars: 200 nm).

Optical characterization

To demonstrate the developed strategy, the feasibility of GO/AuNP complexes as the platform for enhancing the SERS signal of Raman reporters was first investigated. As seen in Fig. 3a, there was no SERS signal for native AuNPs. After conjugation with Raman reporter MGITC, the resulting MGITC modified AuNPs showed an obvious SERS signal (Fig. 3b). Then after further conjugation with antibodies, the SERS signal was almost the same as that of the MGITC modified AuNPs (Fig. 3c). Meanwhile, if the antibody/MGITC functionalized AuNPs conjugated with GO, the Raman intensity was significantly enhanced (Fig. 3d), which indicated the extraordinary SERS enhancement capacity of the designed GO/AuNP

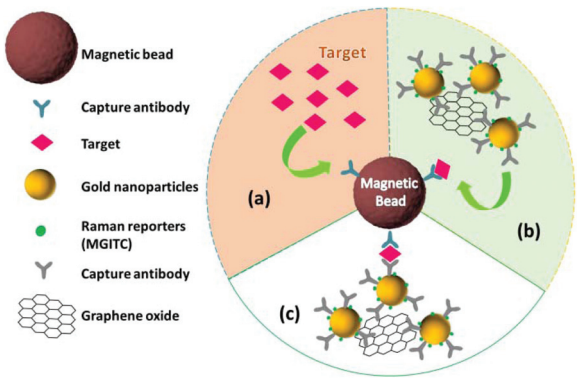

Fig. 1 Schematic illustration of the GO/AuNP-based signal amplification SERS strategy for quantification of cTnI. (a) Target cTnI reacts with the capture probe (antibody-functionalized magnetic bead); (b) the resulting capture probe/cTnI conjugates react with SERS nanotags; and (c) the formed capture probe/cTnI/SERS nanotag immunocomplex.

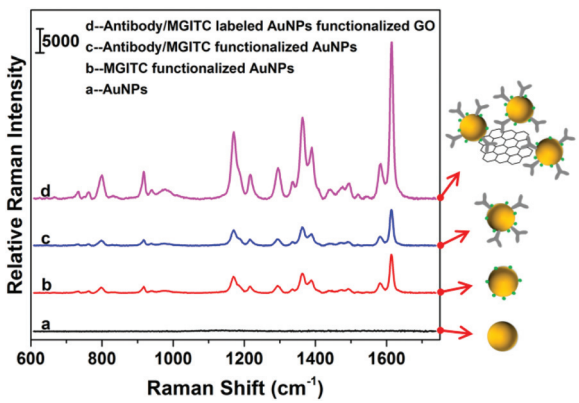

Fig. 3 Raman spectra of the developed GO/AuNP-based SERS immunoassay for different conditions: (a) AuNPs, (b) MGITC functionalized AuNPs, (c) antibody/MGITC functionalized AuNPs, and (d) antibody/MGITC labeled AuNP–functionalized GO.

complexes. All these results were consistent with our anticipated results and confirmed the feasibility of the SERS assay for detection of cTnI.

Optimization of experimental parameters

In order to acquire an optimal analytical performance, the experimental conditions for this signal amplification SERS immunoassay should be optimized. Among these conditions, the volume ratio of antibody/MGITC functionalized AuNPs (AAM) to GO was very crucial since it directly affected the sensitivity of SERS immunoassay. Thus, the volume ratio of AAM to GO and the Raman intensity were investigated and the corresponding results are shown in Fig. S4A.† It could be seen that the Raman intensity gradually increased in the volume ratio of 1 : 0–150 : 1, which was because of the increased amount of AAM on one GO sheet. At volume ratios >150 : 1, the change in the Raman intensity was not obvious, which was probably due to the fact that AAM on the surface of GO were close to saturation. Therefore, the optimal volume ratio of AAM and GO was chosen as 150 : 1.

Next, the influence of the volume ratio of the capture probe (antibody-functionalized magnetic bead, MBA) to SERS nanotags (antibody/Raman reporter labeled AuNP–functionalized GO, GAAM) on the SERS intensity was investigated with ten different volume ratios (Fig. S4B†). It was found that the SERS signal became large with the increase in the volume of SERS nanotags in the range of 1 : 0 to 1 : 3.5 because of the increase in the conjugated amount of SERS nanotags on the surface of the capture probe. However, further increasing the volume ratio of SERS nanotags could not cause any significant change in the Raman intensity, which might be ascribed to the fact that no binding sites remained on the surface of the capture probe; this implied that the Raman intensity tended to reach saturation. Therefore, the volume ratio of 1 : 3.5 was used in this work.

Finally, we studied the incubation time of the capture probe/cTnI conjugates and SERS nanotags for detection of cTnI. Specifically, we measured the Raman intensities for a range of incubation times (10, 20, 30, 40, 50, 60, 70, 80, 90, and 100 min). As seen from Fig. S4C,† the SERS intensity increased rapidly with the reaction time increasing up to 60 min and reached a maximum threshold. This incubation time is much shorter than that of the conventional ELISA method (120 min) due to the significantly enhanced binding probability between the capture probe/cTnI conjugates and SERS nanotags. Thus, 60 min was chosen as the optimal incubation time.

Performance of the SERS sensor

The ability of the developed GO/AuNP-based SERS immunoassay for the quantitative analysis of cTnI was evaluated. Under the above optimized conditions, the Raman spectra of the magnetic immunocomplexes for different concentrations of cTnI were recorded. Fig. 4A illustrates that the SERS intensity gradually increased upon increasing the concentration of cTnI from 0 to 1000 ng mL^{-1}. As the cTnI concentration

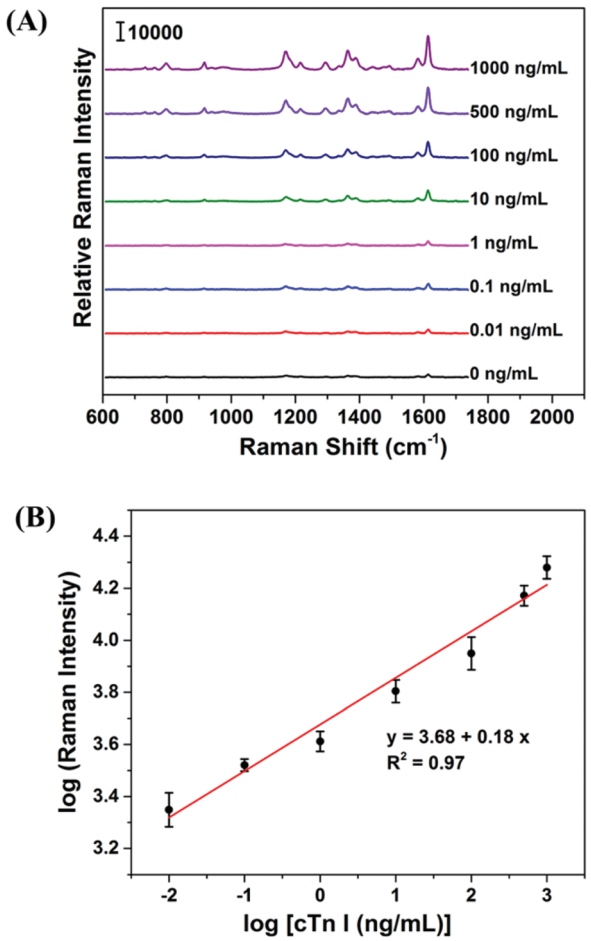

Fig. 4 (A) SERS spectra for cTnI at different concentrations in PBS buffer and (B) the corresponding intensity of the SERS signal at 1613 cm^{-1}. Error bars were obtained from five parallel experiments.

increased, more magnetic immunocomplexes were formed, which means that more SERS nanotags were captured on the surface of antibody-functionalized MB, thus resulting in the SERS intensity increasing accordingly. The relative Raman intensity of MGITC at 1613 cm^{-1} was measured and employed as a quantitative evaluation of the target antigen levels, which is the most intense Raman peak of reporter MGITC. The corresponding calibration plot of the Raman intensity at 1613 cm^{-1} *versus* the target cTnI concentration is displayed in Fig. 4B. For each concentration, the Raman intensities for five different measurements were averaged and the error bars indicated the standard deviation of the five measurements. In this figure, a linear curve was obtained *via* log–log transformation, which exhibited a good linear response in the range of 0.01–1000 ng mL^{-1}. The limit of detection (LOD) value was estimated to be 5 pg mL^{-1}, which was according to the IUPAC standard method ($LOD = y_{blank} + 3 \times SD_{blank}$, y_{blank} is the average signal intensity of the blank and SD_{blank} is the standard deviation of the blank measurements). This value is much lower than the cut-off concentrations of cTnI (0.6 ng mL^{-1}) in serum for diagnosis of AMI[44] and lower than those of

the reported enzyme-linked immunosorbent assay, fluorescence immunoassay, chemiluminescence immunoassay, colorimetric immunoassay, electrochemistry and pressure methods for cTnI detection as shown in Table S1,† which was attributed to the significant enhancement provided by the multiple signal amplification strategy.

Method performance comparison

To demonstrate the applicability of the developed strategy with high sensitivity, we compared its analytical performance with that of the method without GO only using antibody/MGITC labeled AuNPs as the SERS tags. For this comparison, six different concentrations of cTnI, ranging from 1 to 1000 ng mL^{-1}, were prepared. As illustrated in Fig. S5,† the minimum detectable concentration of the method without GO is 1 ng mL^{-1}, which is 100 times higher than the assay data achieved by our proposed SERS-based immunoassay (0.01 ng mL^{-1}). Furthermore, the detection of a lower concentration range (<1 ng mL^{-1}) is more important for the clinical diagnosis, which means that our SERS-based signal amplification technique is suitable for the early diagnosis of AMI in the clinical laboratory.

Application to SeraSub samples

To investigate the potential clinical application of the proposed GO/AuNP-based SERS immunoassay, cTnI detection in a protein free serum substitute medium (SeraSub) was conducted. In order to mimic real serum conditions, various concentrations of cTnI were spiked into SeraSub solutions and corresponding Raman intensities were measured for quantitative analysis. As shown in Fig. S6A,† remarkable Raman intensities and their changes occurred for the spiked SeraSub with different concentrations of cTnI. Fig. S6B† shows that the Raman intensity at 1613 cm^{-1} gradually increased with an increase in the cTnI concentration range from 0.01 to 1000 ng mL^{-1}. These results indicated that our GO/AuNP-based SERS immunoassay system also works well for cTnI detection in biologically relevant media, which demonstrates that the developed GO/AuNP-based SERS immunoassay has wide applicability to cTnI without significant matrix interference, thus, further proving the great clinical application potential for early diagnosis of AMI.

Specificity of the sensor

The specificity of the proposed GO/AuNP-based SERS immunoassay for cTnI was also investigated in the presence of nonspecific proteins, including human immunoglobulin G (IgG), prostate specific antigen (PSA), carcino-embryonic antigen (CEA) and glucose. Consistent with the expectation, the Raman intensity was greatly increased in the presence of 1 ng mL^{-1} cTnI, while almost no Raman signals were observed for any of the non-specific antigens with a high concentration (100 ng mL^{-1}), as shown in Fig. 5. These results demonstrated that the interaction between the monoclonal antibody on the surface of the magnetic bead and the target antigen is significantly stronger than that between the monoclonal antibody and non-specific antigens. All these results illustrated that this GO/AuNP-based SERS immunoassay possessed excellent specificity and reliability toward the target antigen.

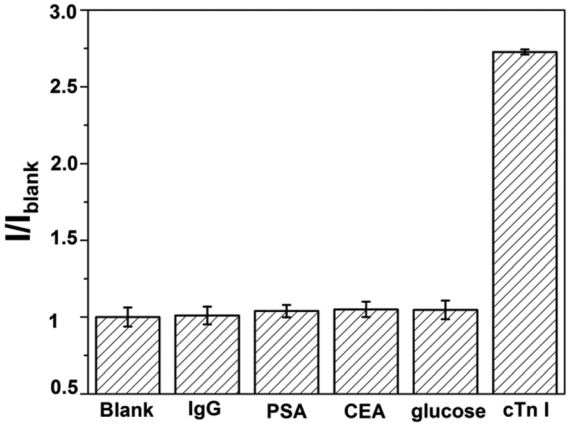

Fig. 5 Relative SERS responses of the GO/AuNP-based SERS immunoassay for cTnI and various nonspecific proteins (I/I_{blank} represents the ratio of the Raman intensity at 1613 cm^{-1}). Error bars indicate the standard deviations of five measurements.

Conclusions

In conclusion, we have successfully developed a novel GO/AuNP-based signal amplification SERS technique, using AuNPs, GO and MB, for highly sensitive quantification of cTnI. Here, monoclonal antibody-conjugated MB and antibody/Raman reporter labeled AuNP–functionalized GO were employed as the capture probe and SERS nanotags, respectively. In the presence of cTnI, the sandwich type complexes, "capture probe/target/SERS nanotags", were formed by antibody–antigen–antibody interactions. Taking advantage of the strong SERS enhancement ability of the designed GO/AuNP complexes and the high binding chance between the target and the GO/AuNP complexes, we successfully attained the highly sensitive detection of cTnI with a detection limit of 5 pg mL^{-1}. This LOD value is much lower than the clinical cut-off value for the diagnosis of AMI disease. Furthermore, in order to assess the detection sensitivity of our developed strategy, the performance of this work was also compared with those obtained by the method without GO. However, for the method without GO, it was difficult to quantify cTnI at concentrations lower than 1 ng mL^{-1}, demonstrating that our designed GO/AuNP-based signal amplification SERS strategy allows for highly sensitive quantification of cTnI. In addition, this assay can be constructed with different kinds of antibodies and Raman reporters, and thus can be easily used for simultaneous detection of multiple biomarkers. Therefore, this proposed SERS-based signal amplification technique shows strong potential for the clinical diagnosis of AMI disease.

Conflicts of interest

There are no conflicts to declare.

Acknowledgements

This work was financially supported by the National Natural Science Foundation of Shandong Province in China (grant no. ZR2017BB026), the National Natural Science Foundation of China (grant no. 21705139, 21275158, and 21575159), and the Shandong Provincial Natural Science Foundation (No. ZR2014BL031), China.

References

1 M. F. M. Fathil, M. K. Md Arshad, S. C. B. Gopinath, U. Hashim, R. Adzhri, R. M. Ayub, A. R. Ruslinda, M. M. N. Nuzaihan, A. H. Azman, M. Zaki and T.-H. Tang, *Biosens. Bioelectron.*, 2015, **70**, 209–220.
2 N. K. Bakirhan, G. Ozcelikay and S. A. Ozkan, *J. Pharm. Biomed. Anal.*, 2018, **159**, 406–424.
3 G. Lee, R. Twerenbold, Y. Tanglay, T. Reichlin, U. Honegger, M. Wagener, C. Jaeger, M. R. Gimenez, T. Hochgruber, C. Puelacher, M. Radosavac, P. Kreutzinger, F. Stallone, P. Hillinger, L. Krivoshei, T. Herrmann, R. Mayr, M. Freese, D. Wild, K. M. Rentsch, J. Todd, S. Osswald, M. J. Zellweger and C. Mueller, *Am. Heart J.*, 2016, **173**, 8–17.
4 B. Rezaei, M. Ghani, A. M. Shoushtari and M. Rabiee, *Biosens. Bioelectron.*, 2016, **78**, 513–523.
5 A. Qureshi, Y. Gurbuz and J. H. Niazi, *Sens. Actuators, B*, 2012, **171–172**, 62–76.
6 T. Zhang, N. Ma, A. Ali, Q. Wei, D. Wu and X. Ren, *Biosens. Bioelectron.*, 2018, **119**, 176–181.
7 K. Wildi, H. Singeisen, R. Twerenbold, P. Badertscher, D. Wussler, L. J. J. Klinkenberg, S. J. R. Meex, T. Nestelberger, J. Boeddinghaus, O. Miro, F. J. Martin-Sanchez, B. Morawiec, P. Muzyk, J. Parenica, D. I. Keller, N. Geigy, E. Potlukova, Z. Sabti, N. Kozhuharov, C. Puelacher, J. D. de Lavallaz, M. R. Gimenez, S. Shrestha, G. Marzano, K. Rentsch, S. Osswald, T. Reichlin and C. Mueller, *Int. J. Cardiol.*, 2018, **270**, 14–20.
8 C. Trambas, J. W. Pickering, M. Than, C. Bain, L. Nie, E. Paul, A. Dart, A. Broughton and H. G. Schneider, *Clin. Chem.*, 2016, **62**, 831–838.
9 M. Negahdary, M. Behjati-Ardakani, N. Sattarahmady, H. Yadegari and H. Heli, *Sens. Actuators, B*, 2017, **252**, 62–71.
10 G. S. Bodor, S. Porter, Y. Landt and J. H. Ladenson, *Clin. Chem.*, 1992, **38**(11), 2203–2214.
11 G. S. Lim, S. M. Seo, S. H. Paek, S. W. Kim, J. W. Jeon, D. H. Kim, I. H. Cho and S. H. Paek, *Sci. Rep.*, 2015, **5**, 14848.
12 M. M. Vdovenko, N. A. Byzova, A. V. Zherdev, B. B. Dzantiev and I. Y. Sakharov, *RSC Adv.*, 2016, **6**, 48827–48833.
13 S. W. Kim, I. H. Cho, J. N. Park, S. M. Seo and S. H. Paek, *Sensors*, 2016, **16**, 669.
14 N. Sirkka, A. Lyytikäinen, T. Savukoski and T. Soukka, *Anal. Chim. Acta*, 2016, **925**, 82–87.
15 S. Y. Song, Y. D. Han, K. Kim, S. S. Yang and H. C. Yoon, *Biosens. Bioelectron.*, 2011, **26**, 3818–3824.
16 G. Z. Liu, M. Qi, Y. Zhang, C. M. Cao and E. M. Goldys, *Anal. Chim. Acta*, 2016, **909**, 1–8.
17 L. Tang, J. Casas and M. Venkataramasubramani, *Anal. Chem.*, 2013, **85**, 1431–1439.
18 Q. Wu, S. Li, Y. Sun and J. N. Wang, *Microchim. Acta*, 2017, **184**, 2395–2402.
19 G. S. Dorraj, M. J. Rassaee, A. M. Latifi, B. Pishgoo and M. Tavallaei, *J. Biotechnol.*, 2015, **208**, 80–86.
20 S. Lee, D. H. Kwon, C. Y. Yim and S. M. Jeon, *Anal. Chem.*, 2015, **87**, 5004–5008.
21 J. Chao, Z. H. Li, J. Li, H. Z. Peng, S. Su, Q. Li, C. F. Zhu, X. L. Zuo, S. P. Song, L. H. Wang and L. H. Wang, *Biosens. Bioelectron.*, 2016, **81**, 92–96.
22 W. H. Wu, J. Li, D. Pan, J. Li, S. P. Song, M. G. Rong, Z. X. Li, J. M. Gao and J. X. Lu, *ACS Appl. Mater. Interfaces*, 2014, **6**, 16974–16981.
23 S. Zhang, N. Huang, Q. J. Lu, M. L. Liu, H. T. Li, Y. Y. Zhang and S. Z. Yao, *Biosens. Bioelectron.*, 2016, **77**, 1078–1085.
24 Q. Zhou, G. H. Li, Y. J. Zhang, M. Zhu, Y. K. Wan and Y. F. Shen, *Anal. Chem.*, 2016, **88**, 9830–9836.
25 Y. M. Si, Z. Z. Sun, N. Zhang, W. Qi, S. Y. Li, L. J. Chen and H. Wang, *Anal. Chem.*, 2014, **86**, 10406–10414.
26 R. Li, S. Y. Li, M. M. Dong, L. Y. Zhang, Y. C. Qiao, Y. Jiang, W. Qi and H. Wang, *Chem. Commun.*, 2015, **51**, 16131–16134.
27 H. Wang, S. Li, Y. M. Si, N. Zhang, Z. Z. Sun, H. Wu and Y. H. Lin, *Nanoscale*, 2014, **6**, 8107–8116.
28 H. Wang, S. Li, Y. M. Si, Z. Z. Sun, S. Y. Li and Y. H. Lin, *J. Mater. Chem. B*, 2014, **2**, 4442–4448.
29 R. K. Gao, Z. Y. Cheng, X. K. Wang, L. D. Yu, Z. Y. Guo, G. Zhao and J. B. Choo, *Biosens. Bioelectron.*, 2018, **119**, 126–133.
30 Z. Y. Cheng, N. Choi, R. Wang, S. Lee, K. C. Moon, S. Y. Yoon, L. X. Chen and J. B. Choo, *ACS Nano*, 2017, **11**, 4926–4933.
31 R. Wang, H. Chon, S. Lee, Z. Y. Cheng, S. H. Hong, Y. H. Yoon and J. B. Choo, *ACS Appl. Mater. Interfaces*, 2016, **8**, 10665–10672.
32 X. L. Fu, L. X. Chen and J. B. Choo, *Anal. Chem.*, 2017, **89**, 124–137.
33 K. Kneipp, H. Kneipp, I. Itzkan, R. R. Dasari and M. S. Feld, *Chem. Rev.*, 1999, **99**, 2957–2976.
34 Y. Q. Wang, B. Yan and L. X. Chen, *Chem. Rev.*, 2013, **113**, 1391–1428.
35 X. L. Fu, Z. Y. Cheng, J. M. Yu, P. Choo, L. X. Chen and J. B. Choo, *Biosens. Bioelectron.*, 2016, **78**, 530–537.

36 P. C. Lee and D. Meisel, *J. Phys. Chem.*, 1982, **86**, 3391–3395.
37 X. L. Fu, L. X. Chen, J. H. Li, M. Lin, H. Y. You and W. H. Wang, *Biosens. Bioelectron.*, 2012, **34**, 227–231.
38 D. R. Dreyer, S. Park, C. W. Bielawski and R. S. Ruoff, *Chem. Soc. Rev.*, 2010, **39**, 228–240.
39 P. Sharma, S. K. Tuteja, V. Bhalla, G. Shekhawat, V. P. Dravid and C. R. Suri, *Biosens. Bioelectron.*, 2013, **39**, 99–105.
40 G. Frens, *Nat. Phys. Sci.*, 1973, **241**, 20–22.
41 G. T. Hermanson, *Bioconjugate Techniques*, Academic Press, Amsterdam, The Netherlands, 2nd edn, 2008.
42 D. Du, L. M. Wang, Y. Y. Shao, J. Wang, M. H. Engelhard and Y. H. Lin, *Anal. Chem.*, 2011, **83**, 746–752.
43 L. M. Zhang, J. G. Xia, Q. H. Zhao, L. W. Liu and Z. J. Zhang, *Small*, 2010, **6**, 537–544.
44 M. J. Tanasijevic, C. P. Cannon, D. R. Wybenga, G. A. Fischer, C. Grudzien, C. M. Gibson, J. W. Winkelman, E. M. Antman and E. Braunwald, *Am. Heart J.*, 1997, **134**(4), 622–630.